Analysis of biomass hydrothermal liquefaction and biocrude-oil upgrading for renewable jet fuel production

The impact of reaction conditions on production costs and GHG emissions performance

Tzanetis, Konstantinos F.; Posada, John A.; Ramirez, Andrea

DOI
10.1016/j.renene.2017.06.104

Publication date
2017

Document Version
Final published version

Published in
Renewable Energy

Citation (APA)
Tzanetis, K. F., Posada, J. A., & Ramirez, A. (2017). Analysis of biomass hydrothermal liquefaction and biocrude-oil upgrading for renewable jet fuel production: The impact of reaction conditions on production costs and GHG emissions performance. *Renewable Energy*, *113*, 1388-1398. https://doi.org/10.1016/j.renene.2017.06.104

Renewable Energy 113 (2017) 1388–1398

Contents lists available at ScienceDirect

Renewable Energy

journal homepage: www.elsevier.com/locate/renene

Analysis of biomass hydrothermal liquefaction and biocrude-oil upgrading for renewable jet fuel production: The impact of reaction conditions on production costs and GHG emissions performance

Konstantinos F. Tzanetis [a], John A. Posada [b], Andrea Ramirez [a, *]

[a] Copernicus Institute, Group Energy & Resources, Utrecht University, Heidelberglaan 2, 3584 CS, Utrecht, The Netherlands
[b] Department of Biotechnology, Delft University of Technology, van der Maasweg 9, 2629 HZ, Delft, The Netherlands

ARTICLE INFO

Article history:
Received 28 December 2016
Received in revised form
20 April 2017
Accepted 30 June 2017
Available online 3 July 2017

Keywords:
Bio-oil upgrading
Jet biofuel
GHG emissions
Hydrothermal liquefaction
Lignocellulosic biofuels
Economic evaluation

ABSTRACT

This paper shows a detailed analysis of a biomass HTL process by considering changes in three main reaction variables (*i.e.* catalysts (water, Na_2CO_3(aq.), and Fe(aq.)), temperature (280–340 °C), and catalysts/biomass mass ratio (0–0.33 kg catalysts/kg biomass)), and by assessing their influence on the techno-economic and GHG emissions performance. This analysis is based on Aspen Plus® simulations, process economics and life-cycle GHG assessment on SimaPro (using Ecoinvent 2.2). Results showed that the lowest production cost for biocrude oil is achieved when HTL is performed at 340 °C with Fe as catalyst (450 €/$t_{\text{biocrude-oil}}$ or 13.6 €/$GJ_{\text{biocrude-oil}}$). At these conditions, the biocrude oil produced has an oxygen content of 16.6 wt% and a LHV of 33.1 MJ/$kg_{\text{biocrude-oil}}$. When the hydrotreatment and hydrogen generation units are included, the total production costs was 1040 €/$t_{\text{upgraded-oil}}$ or 0.8 €/$L_{\text{upgraded-oil}}$. After fractionation, the estimated production cost was 1086 €/$t_{\text{biojet-fuel}}$ or 25.1 €/$GJ_{\text{biojet-fuel}}$. This value is twice the commercial price of fossil jet fuel. However, the allocated life cycle GHG emissions for renewable jet fuel were estimated at 13.1 $kgCO_{2\text{-eq.}}$/$GJ_{\text{biojet-fuel}}$, representing only 15% the GHG emission of fossil jet fuel and therefore, indicating a significant potential on GHG emission reduction.

1. Introduction

The aviation sector is one of the fastest growing forms of transportation with an expected annual increase rate of 5% in air traffic until 2030 [1]. By 2020, aviation emissions are projected to be around 70% higher than those of 2005, even if fuel efficiency improves by 2% per year; and by 2050, they could grow by an additional 300–700% [2]. However, in an effort to address climate change concerns, the Air Transport Action Group (ATAG) has set the ambitious goals to first stabilize the net CO_2 emissions of the aviation sector at 2020 levels (through carbon neutral growth) and then, by 2050, reduce the emissions to 50% of those in 2005 [3–6]. To achieve these goals a combination of two basic strategies will be needed: *i*) improving aircraft technology and/or operation efficiency, and *ii*) developing less carbon intensive fuels. In line with the latter, developing low carbon bio-based jet fuel supply chains is essential. However, considering that jet engine technology and existing infrastructure are unlikely to change in the near future, it is necessary to develop a "drop-in" fuel capable of (partly) replacing the fossil jet fuel. In this sense, biojet fuel is regarded as a promising alternative for reducing GHG emissions.

Biojet fuel can be produced from lignocellulosic biomass, carbohydrates, or vegetable oils through several technologies [4,5]: biomass gasification and Fischer-Tropsch synthesis (FT), hydrotreated depolymerized cellulosic jet (HDCJ), direct sugars to hydrocarbons (DSHC), alcohol to jet (ATJ), and hydro-processed esters and fatty acids (HEFA). Among those, HEFA is the most mature technology although it has very high production costs associated with its feedstocks [4]. Similarly, DSHC and ATJ have also been reported to have high production costs mainly related to the use of feedstocks containing sugars or starch [7]. For direct conversion of biomass, FT is the most advanced pathway, but its high operating costs, capital intensity and technological uncertainties make it a difficult investment option in the short term [4,5]. On the other hand, HDCJ has shown good potential in terms of cost reduction despite its relatively high complexity and severe processing conditions [7]. In general, HDCJ technologies such as hydrothermal

---

* Corresponding author. Present address: Faculty of Technology, Policy and Management, Delft University of Technology, The Netherlands.
E-mail address: c.a.ramirezramirez@tudelft.nl (A. Ramirez).

http://dx.doi.org/10.1016/j.renene.2017.06.104

liquefaction (HTL) and pyrolysis have shown low production costs (*i.e.* 21.4 €/GJ (940 €/t) and 30.2 €/GJ (1325 €/t)) as a result of relatively high yields and modest capital costs [4]. In HDCJ, biomass can be converted via either pyrolysis or HTL into a biocrude oil, which needs to be hydro-processed due to its oxygen content and molecular weight in comparison to petroleum crude [8].

In *biomass pyrolysis* (400–600 °C, atmospheric pressure, and 1 s) a liquid bio-oil with an oxygen content of 35–40 wt% and an energy value of 16–19 MJ/kg is generated [8]. However, its high water content (15–30 wt%) results in unwanted properties: low energy density, low flame temperature, and ignition complications [8]. The oxygen content, water level and physicochemical properties of this pyrolysis oil can be adjusted using catalysts to produce a partially deoxygenated and stabilized bio-oil [9]. *Hydrothermal liquefaction* (subcritical state: 280–380 °C and 7–20 MPa for 10–60 min [8]) produces a biocrude oil with lower oxygen content (10–20 wt%) and higher energy value (30–35 MJ/kg) [8,10]. The relatively low oxygen content leads to improved thermal stability and lower associated upgrading costs. Furthermore, HTL is carried out in presence of water, thereby making use of biomass moisture to avoid the high energy- and capital-intensive drying step required in pyrolysis. This HTL process can also be performed by a range of different catalysts, varying from alkaline solutions to solid iron-based materials [11].

The mentioned advantages make HTL an especially attractive technology for further development and improvement of its performance. However, most studies on biojet fuel production have mainly considered highly aggregated data and simple scaling-up factors to compare the techno-economic (and sometimes environmental) performance of different technologies [4,5]. Thus, studies performed on these technologies have reported figures containing large uncertainties, which may have led to optimistic estimations (lower than actually expected) on production costs and potential GHG emissions reduction. Therefore, in this paper we perform an in-depth analysis of the technical, economic and GHG emissions performance of HTL to: *i)* increase accuracy for estimations on biojet fuel production costs and related GHG emissions; and *ii)* identify key challenges and opportunities to support the development of the biojet fuel sector. To do so, we investigate the influence of three main reaction variables (*i.e.* catalysts (water, $Na_2CO_{3(aq.)}$, and $Fe_{(aq.)}$), temperature (280–340 °C), and catalysts/biomass mass ratio (0–0.33)) on the total production costs and life cycle GHG emissions. We also compare the HTL performance to that of the catalytic pyrolysis (CP) given its higher level of development.

2. Methods

A process simulation model for a standalone HTL plant was built using Aspen Plus®, in a two-step sequential procedure, based on experimental data reported in literature. In the first step, production of biocrude oil (from biomass) was modelled and evaluated to assess its techno-economic performance as well as to identify the best operational conditions for key reaction variables (*i.e.* catalysts, temperature, and catalysts/biomass ratio). Next, the biocrude-oil upgrading and steam reforming units were added to the process simulation model as separate modules built in Excel. In the case of the full HTL plant (from biomass to biojet fuel), the techno-economic and life cycle GHG emissions performance were evaluated. Furthermore, a sensitivity analysis was performed to study the effects of key economic parameters on the performance indicators. A similar two-step sequential procedure was followed for the pyrolysis-based process, but in this case only one set of operational parameters was considered. Further details about the used approach are provided in the following subsections.

2.1. Basis of design

The plant was assumed to be located in Sweden given its high biomass availability. A biomass processing capacity of 1000 t (dry biomass) per day was chosen for a typical plant, and forestry residues were considered as feedstock in all cases. The battery limits for the standalone plant includes three main sections (as shown in Fig. 1): biomass slurring, thermochemical conversion of biomass (integrated with heat generation), and upgrading of biocrude-oil (integrated with hydrogen generation). For the CP process, drying is used instead of slurring.

In general terms, biomass is thermochemically converted in the reactor generating a three-phase product stream: liquid, solid and gas. The produced liquid is separated into two phases: biocrude oil and an aqueous phase (water and dissolved organics). The solid residues (char and ash) are separated from the reactor effluent and sent to a furnace for heat generation. The obtained gas phase is flashed to the furnace for additional heat production. The furnace has a two-fold purpose: generate heat for the reactor and eliminate toxic organic compounds. The biocrude oil is then upgraded through hydrotreatment to remove oxygen and increase its energy density. The hydrotreatment output is separated into a gas phase (vented gas) and two liquid phases: the hydrocarbon product (a mix of renewable: jet fuel, gasoline, diesel and heavy oil), and a waste aqueous stream. The biojet fuel fraction is then obtained via distillation. The vented gas is rich in hydrogen, part of which is separated and recycled to the upgrading reactor. The remaining flow is combined with a fed of natural gas (making up for hydrogen deficiency) and then sent to the steam reformer.

2.2. Description of the biomass reaction cases

For HTL, six sets of reaction conditions were analysed and compared against CP (with only one set of reaction conditions). Hence, seven conversion cases for biocrude oil production were developed as shown in Table 1. The six HTL cases are named based on both the used catalyst (*i.e.* 'W' for water, 'NA' for Na_2CO_3, and 'FE' for iron) and the reaction temperature (*i.e.* 280, 300, or 340) as shown in Table 1. For catalytic pyrolysis, the letters 'CP' are used.

The design variables were selected based on the effects of key operating parameters (temperature, pressure, solvent type, catalysts) on the process performance. The review indicated that:

- Liquefaction temperature typically ranges from 280 to 374 °C [8] (subcritical state). High temperatures facilitate the decomposition of polymers into a liquid-rich phase [12]; however, very high temperatures favour gas formation [12,13]. Experimental work showed that in a range of 280–360 °C, oil formation was higher than that of water-soluble oil [14]. Intermediate temperatures (300–350 °C) generally yield higher amounts of bio-oil [12,13], and therefore were more appropriate for HTL.
- Pressure is reported to be around 15 MPa [8,15], thus maintaining single-phase media for subcritical (and supercritical) liquefaction [13]. Relatively high pressure in subcritical liquefaction is reported to favour liquids over gases [12].
- HTL occurs for 10–60 min [8], with shorter residence times producing higher amounts of bio-oil with an effect on bio-oil composition [13].
- Solvents on HTL might have significant effects on yield, however the use of water is here preferred due to its lower cost and higher evaporation temperature compared to alcohols. Furthermore biomass HTL in water can be performed with or without the presence of catalysts; for example, Na_2CO_3 and Fe catalysts have been reported to effectively enhance formation of hydrocarbon and promote gas formation [14].

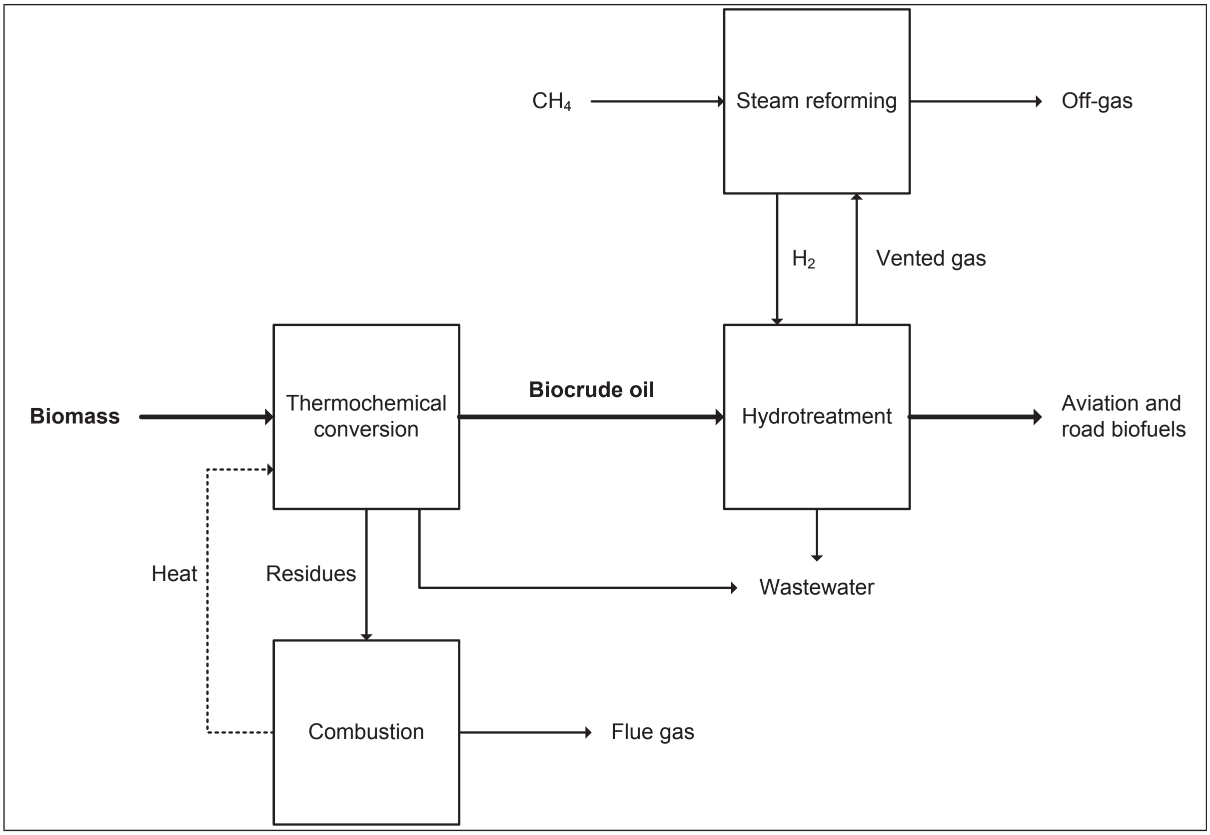

Fig. 1. Simplified process block scheme of biomass to aviation and road biofuels.

Table 1
Biomass reaction cases and processing conditions for HTL and CP.

Case	Technology	Catalyst	Mass concentration ($kg_{catalyst}/kg_{biomass}$ in %)	Temperature (°C)
W280	Hydrothermal liquefaction	Water	–	280
W300	Hydrothermal liquefaction	Water	–	300
NA280	Hydrothermal liquefaction	Na_2CO_3 (aq.)	5	280
NA300	Hydrothermal liquefaction	Na_2CO_3 (aq.)	5	300
FE300	Hydrothermal liquefaction	Fe (aq.)	10	300
FE340	Hydrothermal liquefaction	Fe (aq.)	10	340
CP	Catalytic pyrolysis	Sand-CaO	33	450

The parameters with the strongest effects on the process performance (yield, product distribution, composition) were selected as the key design variables: reaction temperature and liquefaction medium (*i.e.* catalyst and biomass load).

2.3. Simulation approach

Process simulation was performed in Aspen Plus® to generate mass and energy balances. For the developed simulation models, the thermochemical reactor and its operating conditions were considered to be the most relevant factors of the process design. In this case, the operating parameters and yields were selected based on experimental results reported in literature [11,14] (see Table 2). The HTL unit was simulated using a yield reactor model, operated at constant conditions of temperature and pressure. The temperature was varied in the range of 280–340 °C depending on the case (see Table 1). The pressure was set at 15 MPa [15] to keep the reaction in liquid phase. The CP units was simulated using a yield reactor model, operated at constant temperature and pressure (450 °C and 1atm). For biocrude upgrading, a 100% conversion approach was followed since equilibrium calculations predicted full conversion of representative compounds [16]. The modelling of hydrogen generation via steam reforming was based on non-stoichiometric chemical equilibrium reactor with Gibbs free energy minimization [17].

Since the selection of a suitable thermodynamic property method is key to achieve reliable simulation results, several models were tested considering the wide range of components in the HTL system, *i.e.* hydrocarbons, light gases and polar compounds. After several test runs, the Soave-Redlich-Kwong (SRK) property method was found to be capable of both predicting immiscibility of biocrude oil with water, and reproduce results of miscibility and phase separation that were consistent with literature data [14]. However, the non-random two-liquid (NRTL) model was determined to be more suitable to describe the vapour liquid equilibrium (VLE) of the strongly non-ideal system obtained from the liquefaction reactor. Based on the above, the SRK model was selected for all unit operations except the gas-liquid separator, for which the NRTL model was preferred.

The yields implemented in the Aspen Plus® models for HTL and

Table 2
Yields for HTL and CP. Adapted from Refs. [11,14].

Component	Hydrothermal liquefaction						Catalytic pyrolysis
	In water		In Na_2CO_3 $_{(aq.)}$		In Fe $_{(aq.)}$		
	280 °C	300 °C	280 °C	300 °C	300 °C	340 °C	450 °C
Biocrude oil	23.0	27.0	28.0	32.0	28.5	36.0	14.8
Solid residue	23.0	20.0	14.5	8.0	17.5	10.0	26.0
Dissolved organics	17.5	16.0	32.5	31.5	25.0	15.0	12.9
Water	26.5	26.0	9.0	13.0	14.0	21.0	21.4
Gas	10.0	11.0	16.0	15.5	15.0	18.0	25.0

CP are described in Table 2. The compositions of the gas product stream and aqueous phase were assumed to be independent of catalyst presence and type. The biocrude oil is composed of a light and a heavy fraction [18]. The heavy fraction consists of high molecular weight hydrocarbons typically with a boiling point higher than 300 °C. Data on the ratio of light and heavy oil fractions for hydrothermal liquefaction was retrieved from literature [18]. Linear interpolation was applied to adjust those data to the reaction temperatures of the current study. Thus, the weight percentage of the light fraction was calculated as 49.2%, 42.0%, and 40.4% for 280 °C, 300 °C, and 340 °C respectively. The percentage of the light fraction in CP was assumed to be 50%, since no relevant data were publicly available. Furthermore, the composition of the biocrude oil was assumed to be represented by the dominant components of the different functional groups present in each phase according to the experimental characterization data reported in literature [14,19]. The dominant compounds for each fraction and functional group are described in Table 3. Furthermore, an aliphatic compound of high boiling point was selected to represent the heavy biocrude fraction. The composition of the light biocrude was determined by organizing the compounds found in the oil [14] according to their functional group, as listed in Table 3.

2.4. Process description

2.4.1. Hydrothermal liquefaction

The process flow diagram for HTL is shown in Fig. 2A. Biomass is mixed with water resulting in a biomass-water slurry that is pumped to a preheating unit, and then to the liquefaction reactor. The solid residues are removed from the reactor effluent and combusted for heat generation. The furnace inlet airflow rate is determined by the oxygen excess specifications to achieve complete combustion (*i.e.* 5 wt% O_2 in the flue gas [20]). In some cases, additional fuel (*i.e.* natural gas, although additional dried biomass could also be used) is co-fed to the furnace in order to meet the process heat requirements. It is assumed that the combustion takes place in an adiabatic furnace. As a result, all generated heat is transferred to the flue gas, which is used for supplying heat to the reactor. Surplus heat can be recovered as steam before the flue gas is discharged at 150 °C [21].

The hot reactor effluent exchanges heat with the cold reactor feed, thus serving both separation and reaction purposes. The light gases are separated in a flash drum at 90 °C and 1atm to achieve a high recovery efficiency of the light gases fraction. The light gases and a small amount of organic compounds are removed and sent to the furnace to be fully combusted together with the solid residue. The immiscible oil fraction is separated from the aqueous phase in a decanter. The decantation temperature was set at 80 °C to avoid a high water content in the product while ensuring the liquid phase conditions (biocrude oil solidifies below 80 °C) [8]. The separated aqueous phase (containing 1 wt% organics) is recycled at a high ratio (90%) to reduce costs related to wastewater treatment. The most relevant data process inputs and assumptions for biocrude production via HTL are listed in Table 4.

2.4.2. Catalytic pyrolysis

The process flow diagram for CP is shown in Fig. 2B. Biomass is first dried with flue gas coming from the furnace [22] and a moisture up take rate of 5 MJ/kg [23] is assumed. Once the CP reaction has taken place, the resulting solids are separated and combusted for heat generation using the same outlet oxygen specifications as for HTL. The hot effluent is cooled down in a steam generator and sent to the flash drum. The light gases are removed and combusted in the furnace along with the solids. The liquid product is separated into organic and aqueous phases. Heat is recovered from the flue gas to meet the energy requirements of the reactor and drier combined, *i.e.* 2.6 and 5.0 GJ per tonne of dry biomass respectively. The remaining heat can be recovered as

Table 3
Mass composition (in %) of the biocrude oil and organics in aqueous phase for HTL and CP. Model compounds for the Aspen Plus simulation model are included as representative compounds. Adapted from Refs. [14,19].

Phase/Functional group	Representative compound	Hydrothermal liquefaction			Catalytic pyrolysis
		In water	In Na_2CO_3 $_{(aq.)}$	In Fe $_{(aq.)}$	
Biocrude oil					
Light fraction					
Ketones	2-methyl-2-cyclopentene-1-one	21.8	26.6	25.7	20.5
Aliphatic acids	Nonanoic acid	12.9	7.3	6.0	5.4
Aromatics	Trimethoxymethylbenzene	18.5	19.3	11.1	9.8
Furans	2,5-dimethyloxole	3.7	1.2	0.9	8.3
Phenols	Guaiacol	43.1	45.6	56.3	56.0
Heavy fraction	9-octadecenoic acid	100.0	100.0	100.0	100.0
Organics dissolved in aqueous phase					
Acids	Glycolic acid	71.0	71.0	71.0	100.0
Alcohols	Methanol	18.0	18.0	18.0	0.0
Phenols	Phenol	2.0	2.0	2.0	0.0
Ketones	Acetone	9.0	9.0	9.0	0.0

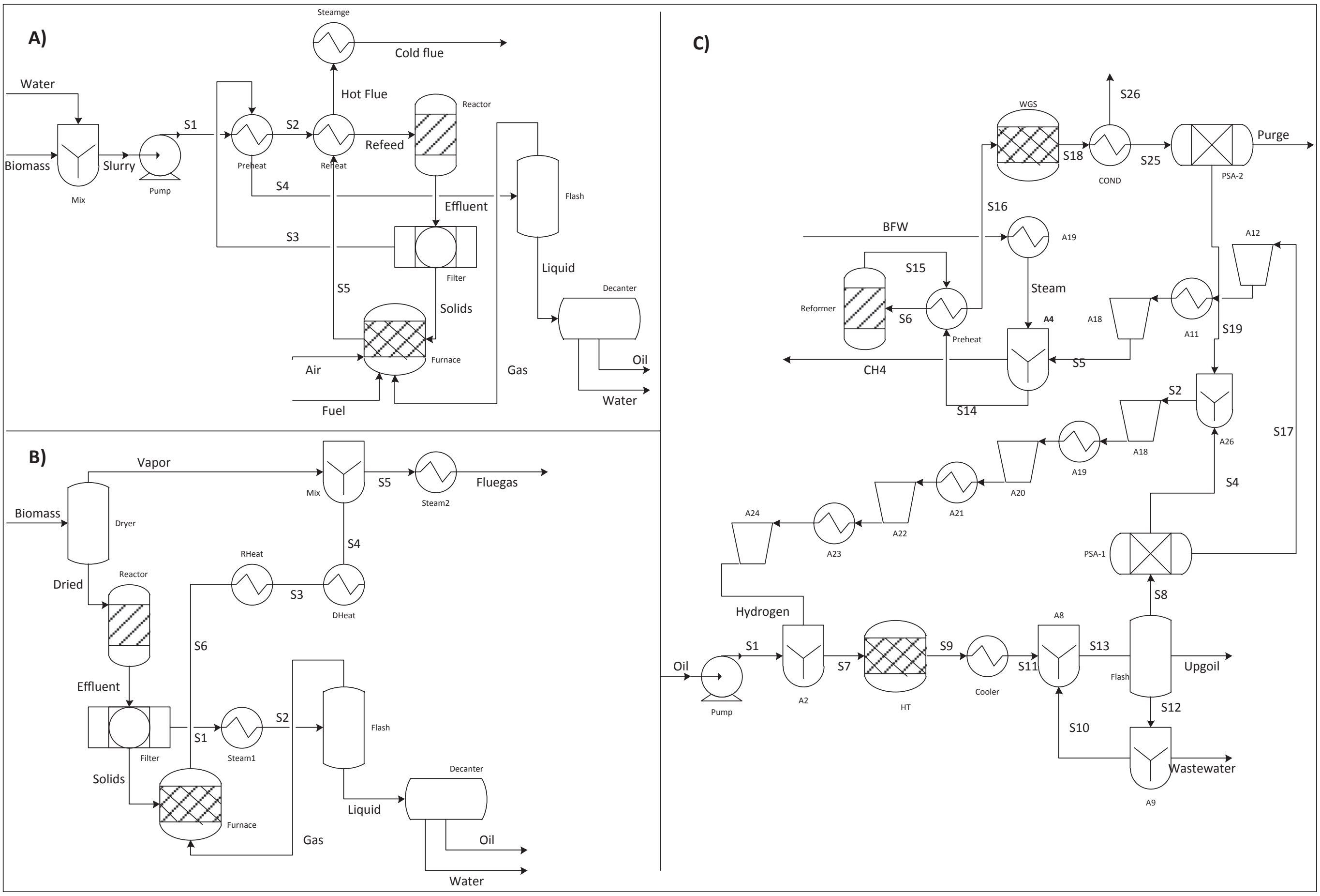

Fig. 2. Process flow diagram for: **A)** hydrothermal liquefaction; **B)** catalytic pyrolysis; and **C)** biocrude-oil upgrading and integrated hydrogen generation.

steam. Since low flash temperatures favour the overall biocrude yield, the flash temperature was set at 35 °C. The decanter temperature was selected to achieve zero cooling or heating requirements. The wastewater stream has a relatively high organic content (~40 wt%), which could be converted into gas rich in CH_4 and CO_2 via anaerobic digestion [24]. The most relevant data process inputs for biocrude production via CP are shown in Table 4.

2.4.3. Biocrude-oil upgrading and integrated hydrogen generation

Biocrude oil derived from thermochemical conversion of biomass is a heavy organic liquid with relatively high oxygen content, which can be upgraded into a conventional hydrocarbon fuel via hydrogen treatment [8,15]. This upgrading process (typically at 250–450 °C and 0.75–30 MPa [16]) has a double effect purpose: remove oxygen and saturate double bonds.

The process flow diagram for biocrude-oil upgrading and integrated hydrogen generation is shown in Fig. 2C. A single stage hydrotreatment configuration was here used. The reactor effluent is cooled down in a steam generator and separated into a gas and two liquid phases. A three-outlet flash was implemented in the model to achieve simultaneous gas and water removal. The removed gas contains unreacted hydrogen that is recovered in a pressure-swing adsorption unit and returned to the upgrading reactor to improve the overall hydrogen conversion. The upgrading reactions considered in the current model (see Table 5) are based on the used representative compounds for the bio-oil compositions as listed in Table 3. Furthermore, it was considered that hydrogen consumption exceeds the stoichiometric requirement at high degrees of deoxygenation, thus the requirement for both complete deoxygenation and saturation is 25 moles H_2 per kg bio-oil [16]. Additionally, assumptions of 80% recovery [27] and 100% purity were made for hydrogen. The hydrogen stream is compressed in a multi-stage compressor with intermediate cooling to avoid excessive temperatures. A significant amount of water (~6 tonnes per tonne of biocrude upgraded) is generated during the reaction with hydrogen. Once water is removed, a fraction of it (80%) is recycled back to the flash unit, where a minimum of 25 wt % of water in the bio-oil is required to achieve an effective phase separation [28].

For the steam reformer unit, the hot outlet exchanges heat with the cold inlet to preheat the feed to 600 °C. The vented gas is compressed in a multi-stage compression with intermediate cooling, similar to the hydrogen stream, and then fed to the reformer. The compressed stream is combined with saturated high-pressure steam at 28 bars and fed to the steam reformer. Natural gas is supplied at a ratio of 1.5% (tonne natural gas per tonne biocrude) to make up for hydrogen deficiency. A large amount of water is condensed after the water-gas shift reaction. Since the upgrading process is exothermic and the steam reforming process is endothermic, heat integration is possible. In the current model, the heat recovered from the hot upgrading reactor effluent was used to generate steam for the reforming reaction. The purge stream, containing hydrogen and a small amount of organics, was used for direct combustion. Its combustion heat was calculated to be sufficient to meet the heat requirements of the steam reformer, (~2 GJ per tonne of biocrude upgraded). Table 6 shows the major data inputs for biocrude upgrading and hydrogen generation.

Table 4
Major inputs and assumptions for biocrude oil production via HTL and CP. Adapted from Refs. [10,11,14].

Parameter, units	Value
Biomass feed flowrate, dry t/d	1000
Moisture content of biomass, wt.%	40.0
Dry biomass composition, wt.% [14]	
Cellulose	46.2
Hemicellulose	27.5
Lignin	25.5
Ash	0.8
Biomass conversion, %	100
Hydrothermal liquefaction [14]	
Dry biomass in slurry, wt%	16.7
Temperature, °C	280–340 °C
Pressure, MPa	15[a]
Residence time, min	10
Gas composition, wt.% [10]	
CO_2	94.2
CO	4.7
CH_4	1.0
H_2	0.1
Catalytic pyrolysis [11]	
Moisture content after drying, wt%	1.0
Temperature, °C	450
Pressure, MPa	0.1
Residence time, min	7
Gas composition, wt.% [11]	
CO_2	51.4
CO	39.0
CH_4	9.1
H_2	0.5

[a] The pressure was set to 180 MPa for FE340.

2.5. Technical performance analysis

The process performance indicators used for evaluating both the biomass to biocrude oil, and the biomass to renewable jet fuel process are:

i) *Overall yield of final liquid fuel:* Liquid fuel production output (*i.e.* biocrude oil or upgraded oil) with respect to the dry biomass inlet.
ii) *Quality of the final liquid product:* associated to the heating value and oxygen content (on a dry mass basis). The HHV of biomass, biocrude oil, and upgraded oil is calculated using the Dulong formula: $\text{HHV (MJ/kg)} = 0.338\,C + 1.428\,(H - O/8)$ [18]. The LHV can be calculated considering the hydrogen and moisture content of the fuel: $\text{LHV} = \text{HHV} - 2.4 \times 8.9\,H$, where 2.4 kJ/kg is the vaporization latent heat of water (considering heat capacity differences between liquid and gas phases) and 8.9 is the stoichiometric coefficient (for water formation per gram of hydrogen in the fuel).
iii) *Energy efficiency of the process:* Defined as the energy output (biocrude oil or upgraded oil) divided by the total energy input (biomass, natural gas, and electricity). Electricity was converted into primary energy using an energy conversion efficiency factor of 40%. For biomass, HHV and LHV were estimated to be 15.6 and 14.2 MJ/kg respectively [18].

Table 5
Biocrude-oil upgrading reactions assumed by organic groups based on model compounds. Adapted from Refs. [16,25,26].

Organic groups	Assumed reaction (based on model compounds)
Ketones	$C_6H_8O + 3H_2 \rightarrow C_6H_{12} + H_2O$
Aliphatic acids	$C_9H_{18}O_2 + 3H_2 \rightarrow C_9H_{20} + 2H_2O$
Furans	$C_6H_8O + 3H_2 \rightarrow C_6H_{12} + H_2O$
Aromatics	$C_{10}H_{14}O_3 + 6H_2 \rightarrow C_{10}H_{20} + 3H_2O$
Phenols	$C_7H_8O_2 + 5H_2 \rightarrow C_7H_{14} + 2H_2O$
Heavy biocrude	$C_{18}H_{34}O_2 + 3H_2 \rightarrow C_{18}H_{36} + 2H_2O$
Acids	$C_2H_4O_3 + 2H_2 \rightarrow C_2H_6O_2 + H_2O$
Phenols	$C_6H_6O + 4H_2 \rightarrow C_6H_{12} + H_2O$
Ketones	$C_3H_6O + 2H_2 \rightarrow C_3H_8 + H_2O$

Table 6
Major inputs and assumptions for biocrude oil upgrading and hydrogen generation.

Parameter, Units	Value
Upgrading [16,25]	
H_2 consumption, mole/kg oil	25
Temperature, °C	400
Pressure, MPa	0.85
Conversion, %	100
Hydrogen generation [17]	
Steam reforming	
Temperature, °C	900
Pressure, MPa	2.5
Water gas shift	
Temperature, °C	210
Pressure, MPa	2.5
Conversion, %	100

2.6. Economic evaluation

The economic evaluation was based on the equipment, materials and energy consumption. The capital cost of major equipment (preheater (for HTL), drier (for CP), reactor, furnace) was calculated using equations for purchased costs as function of equipment size factors [29]. The contribution of the remaining equipment (*i.e.* pumps, blower, flash drum, and decanter) was estimated to represent 10% of the total major equipment cost. For the liquefaction unit, a plug flow reactor was selected given its economic and energy efficiency advantages over other reactor configurations [24]. The reactor was assumed to be of shell-and-tube design with slurry in the tubes [24], and its cost was estimated based on its surface area and design factors [29]. The reactor volume was calculated using based on the residence time and volumetric flowrate. The number of tubes and surface area were calculated using a tube diameter of 25 mm and a tube length of 6 m [29]. The purchased equipment costs for the upgrading facility and hydrogen plant were estimated based on the costs of earlier projects [15] using the six-tenth rule [30].

The fixed and total capital investments were estimated using the Lang factor [30]. The various cost elements associated with the production cost are shown in Table 7. Utility and catalyst consumption were calculated from the mass and energy balances. The calculated costs were updated to 2014 costs using the Chemical Engineering Plant Cost Index (CEPCI). When necessary, the costs were converted to € using an exchange rate of 0.75 €/$\$_{2014}$. For calculating labour costs, two operators for each major process step and 5 shifts were considered [31,32].

To simplify the analysis, it was assumed that the catalyst is recovered after reaction with 3% losses and with full replacement once a year. Furthermore, for wastewater treatment costs, direct costs factors were used (see Table 7).

The discount rate and project lifetime were assumed as 10% and 20 years, respectively. Finally, the production costs were proportionally allocated to the outputs based on the market price (618€/t (gasoline), 526€/t (diesel), 546€/t (jet fuel) and 460€/t (heavy oil) [33],[1]) and product distribution (24% gasoline, 40% jet fuel, 14%

---

[1] Petroleum gasoline, diesel and heavy oil prices refer to New York Harbour Spot Prices FOB. Petroleum jet fuel price refers to U.S. Gulf Coast Kerosene-Type Jet Fuel Spot Price FOB [33]. The densities for converting to €/t were assumed 0.74, 0.80, 0.83 and 0.92 kg/L for gasoline, jet fuel, diesel and heavy oil, respectively.

Table 7
Parameters and values of the variable costs in the economic model.

Parameter, unit	Value	Units
Operating hours per year	8000	
Lang factor [30]	5.04	For FCI[a]
	5.93	For TCI[b]
Working capital [30]	15%	of TCI
Labour [36],[c]	80000	€/y per employee
Supervision [30]	20%	of labour cost
Maintenance [30]	6%	of FCI
Local taxes [30]	1%	of FCI
Insurance [30]	1%	of FCI
Capital charge[d]	12%	of FCI
Plant overhead [30]	70%	of L, S, and M[e]
Feedstocks		
Forestry residue [4]	95	€/dry tonne
Natural gas [37]	135	€/t
Utilities		
Electricity [38],[f]	70	€/MWh
Cooling water [29]	1	€/MWh
Wastewater treatment [29]	380	€/t org. removed
Catalysts [39]		
Na_2CO_3	150	€/t
Fe	600	€/t
CaO	100	€/t

[a] Fixed Capital Investment.
[b] Total Capital Investment.
[c] 40 €/h and 2000 h/y were considered.
[d] Capital charge factor was calculated using an interest rate of 10% and a project life of 20 years.
[e] Labour, supervision and maintenance.
[f] Electricity price for medium size industries.

diesel and 22% heavy oil on a mass basis [34]). The biofuel prices were converted to €/GJ using specific LHVs: 42.9, 43.2, 43.0 and 39.0 MJ/kg for gasoline, jet fuel, diesel and heavy oil respectively [35].

2.7. Life cycle GHG emissions assessment

For the life cycle GHG emissions assessment, only the two most promising cases identified in the economic evaluation were considered. This part of the analysis aims to: *i*) determine the potential emissions reduction with respect to its fossil counterpart; *ii*) recognize hotspots areas and major GHG emissions contributors, and *iii*) identify areas for further research and development.

The GHG emissions assessment is performed according to ISO 14040 and ISO 14044 standards [40,41], with global warming potential (GWP) as the impact category considered. A cradle-to-grave approach was selected for the system boundaries as shown in Fig. 3.

The functional unit was 1 GJ ^{LHV} of jet fuel produced. The life cycle inventory (LCI) data was generated based on the results of the Aspen Plus® simulation models. An inventory containing the most relevant mass and energy flows was built from the simulation results (see Sections 3.1. and 3.2.). In this study, the biogenic carbon was considered to be CO_2 neutral. Current issues regarding the carbon neutrality of biomass due to indirect land use and carbon debt are not included in the analysis as there is not yet consensus from a methodological point of view, and data is not available [42]. The GHG emission factors and the most relevant aspects of the biomass supply chain for biojet fuel production are shown in Table 8. The emissions related to the catalyst life cycle were not considered since no reliable data about its commercial production were publicly available. Given that the biojet fuel production process is a multifunctional system, the total GWP impacts can be allocated to the multiple products, *i.e.* gasoline, jet fuel, diesel, heavy oil. There are several approached to allocate the impacts, *e.g.* based on their energy content, mass flow, or market price. In this paper, economic allocation is applied. Although for some biorefinery systems the GHG performance has shown to be highly sensitive to the allocation approach, in our case, the energy content and the price of the multiple products are closely related, therefore leading to only minor differences on the allocation factors for a mass-based, energy-based or price-based allocation, see comparison of allocation factors in Table 9.

2.8. Sensitivity analysis

A sensitivity analysis was performed to analyse the effect of two factors with high variability on the economic performance: *i)* biomass feedstock price and *ii)* equipment cost for biocrude production. Thus, in order to analyse their influence on the overall economic performance of biojet fuel production, these two parameters were varied in the range ±50%.

3. Results and discussion

3.1. Techno-economic performance of biocrude oil production

The most important technical performance results for biocrude oil production are shown in Table 10. The highest overall biomass-to-biocrude oil yields are achieved at high temperatures, and in presence of catalysts. In CP, formation of solid and gaseous by-products is favoured over liquids and, therefore, the overall biocrude oil yield is much lower compared to HTL. Furthermore, the energy efficiency of the biocrude oil process, calculated on a LHV basis, ranges from 36 to 89%. The major heat losses are observed in the flue gas and wastewater streams. When steam generation from excess heat is excluded, the energy efficiency is directly proportional to the biocrude yield. However, when steam generation is included, the NA280 and NA300 cases show the lowest energy efficiencies among the HTL cases due to the very low solid residue production since a CO_2-rich gas residue is produced instead. Similarly, in the CP case, the flue gas carries a significant amount of heat (mainly from biomass moisture). Furthermore, a significant amount of organic matter ends up in the wastewater, which could potentially improve the energy efficiency of biocrude production.

The large differences in excess heat could be explained by the differences in liquefaction temperatures, process heat requirements, and solid residue yields. Although the NA300 and FE340 cases require natural gas to fulfil their heat requirements to heat up the hot stream to the required level for effective heat transfer, they also produce excess heat but of low quality.

The results of the economic analysis for biocrude oil production are summarized in Table 10. The total production costs vary mainly due to the high dependence on the biocrude oil yield, which depends on the used catalyst and operating temperature. The total production costs per unit of biocrude oil are higher than that of the fossil crude oil price. The biocrude oil production cost was here estimated in the range 13–35 €/GJ (or 450–1135 €/t) compared to 9.4 €/GJ (or 403 €/t) for fossil crude oil price [33]. The highest contribution to the total production costs comes from biomass feedstock (55–60%) followed by capital charge (15–20%). Thus, the two best cases considering the technical and economic performance are: *i*) FE340 (with the highest biocrude oil yield and the lowest total production costs), and *ii*) W300 (with high biocrude oil yield, low total production costs, and zero requirements of catalyst and natural gas).

3.2. Techno-economic performance of renewable jet fuel production from biomass

Table 11 shows the most important results of the technical

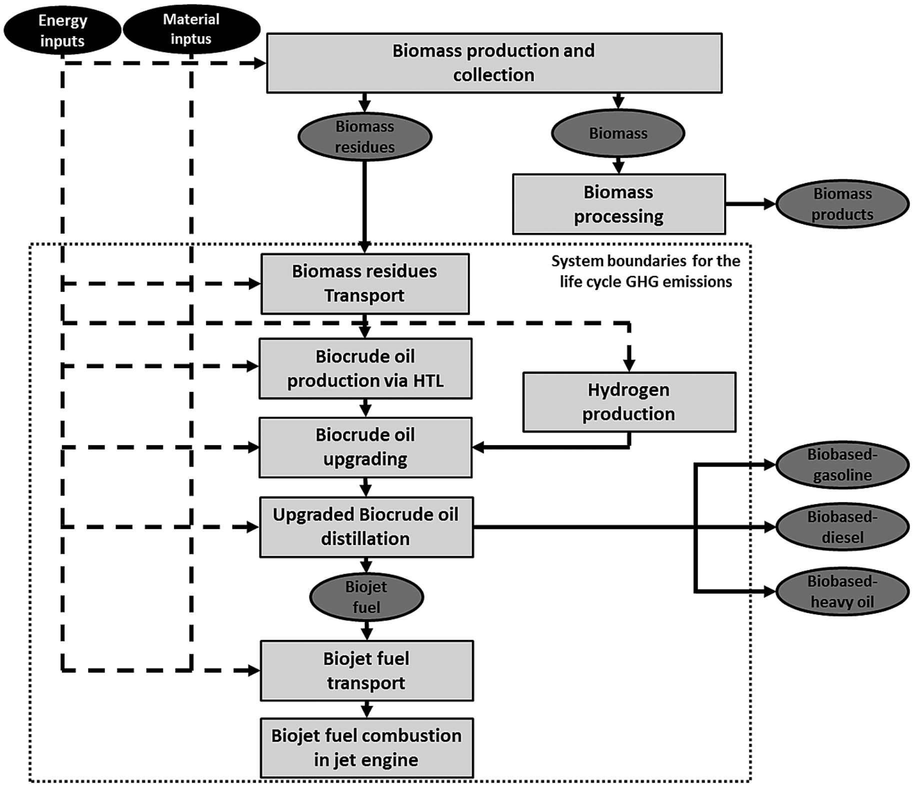

Fig. 3. System boundaries for assessing the GHG performance.

analysis for the two best cases selected in Section 3.1. FE340 has a higher overall upgraded oil-to-biomass yield and a more favourable heat balance than W300 (despite the higher natural gas consumption of FE340). However, if steam generation from excess heat is considered, the energy efficiency of W300 becomes slightly better. The LHV of upgraded oil was calculated at 46.2 MJ/kg, which is 10% higher than its fossil counterpart assuming the same product basket (see Section 2.6).

Table 12 shows the composition of the total production costs FE340 and W300. The total equipment cost is higher for FE340 due to its overall larger processing capacity. Furthermore, the major equipment cost drivers are the liquefaction reactor and the hydrogen plant with around 40% each (see Table 12), and then the upgrading facility with an average contribution of 19%. In both HTL cases, biomass feedstock appears as the major contributor to the production costs with a 34% for FE340 and 38% for W300; followed by capital charge (25–26%) and maintenance costs (13%). The production cost per unit of upgraded oil was calculated to be 0.80 €/L for FE340, and 0.96 €/L for W300; which is in line with data previously ported for HTL of woody biomass (0.56–0.97 € $_{2014}$/L $_{\text{product mix}}$) [24]. Furthermore, the energy allocated biojet fuel production costs here calculated for HTL (25.1 €/GJ$_{\text{biojet-fuel}}$ for FE340 and 30 €/GJ$_{\text{biojet-fuel}}$) are higher than those reported [4] for the same technology (21 €/GJ$_{\text{biojet-fuel}}$), but lower or comparable to those reported for HEFA, FT, pyrolysis, and ATJ (29, 38, 30, 52 €/GJ$_{\text{biojet-fuel}}$, respectively). However, in all cases, the allocated biojet fuel production cost is higher than from petroleum (12.21 €/GJ$_{\text{jet-fuel}}$) [4].

Table 8
Emission factors and most relevant aspects of the biomass supply chain used in the life cycle GHG emissions analysis.

Parameter	Value	Units
Emission factors [a]		
Residual wood[b]	10	$kg_{CO2\text{-}eq}/m^3$
Electricity $_{\text{Sweden}}$	42.4	$kg_{CO2\text{-}eq}$/MWh
Electricity $_{\text{Europe}}$	502	$kg_{CO2\text{-}eq}$/MWh
Heat generation[c]	280	$kg_{CO2\text{-}eq}$/MWh
Hydrogen production[d]	7770	$kg_{CO2\text{-}eq}/t_{\text{hydrogen}}$
Steam generation[e]	234	$kg_{CO2\text{-}eq}/t_{\text{steam}}$
Truck	0.12	$kg_{CO2\text{-}eq}$/t-km
Tank truck	0.19	$kg_{CO2\text{-}eq}$/t-km
Distances		
Forest to HTL plant	100	km
HTL plant to airport	200	km
Capacities		
Truck [43]	40	$t_{\text{woodchips}}$
Tank truck	26.5	$t_{\text{liquid fuel}}$

[a] Data from SimaPro 7.3: Ecoinvent.
[b] Softwood, under bark (wet); density = 0.43 t/m^3 (Norwegian spruce).
[c] From natural gas in a low-NO$_X$ industrial furnace.
[d] From natural gas via SMR.
[e] Steam for chemical processes, at plant.

3.3. *Life cycle GHG emissions performance for renewable jet fuel production*

The allocated GWP results of the biojet fuel production chain (*i.e.* cradle-to-grave considering combustion as the end-of-life

Table 9
Allocation factors for multiple allocation approaches.

Product	Mass allocation	Energy allocation	Economic allocation
Gasoline	24.0%	24.4%	27.7%
Jet fuel	40.0%	41.0%	39.2%
Diesel	14.0%	14.3%	14.2%
Heavy oil	22.0%	20.3%	18.9%

Table 10
Technical and economic performance results for biomass to biocrude oil production.

Parameter, Unit	W280	W300	NA280	NA300	FE300	FE340	CP
Technical performance indicators							
Overall biomass to biocrude yield, %	24.7	28.6	30.5	34.5	30.6	37.5	15.0
Biocrude oil output, t/y	82333	95333	101667	115000	102000	125000	50000
Natural gas consumption, t/y	0	0	0	4600	0	1600	0
Excess heat, MW	50.0	39.1	12.3	3.3	22.7	5.5	35.0
Energy efficiency, %	58	69	71	79	71	89	36
Biocrude oil quality							
HHV, MJ/kg	34.3	35.2	34.1	35.0	34.1	35.2	34.5
LHV, MJ/kg	32.2	33.1	32.0	32.9	32.0	33.1	32.4
Oxygen content, wt.%	17.6	16.7	18.1	17.1	17.9	16.6	17.7
Water content, wt.%	1.3	1.2	1.4	1.2	1.4	1.2	0.6
Economic performance indicators							
Capital costs, k€							
Delivered equipment	14400	14200	12800	12200	13800	15700	17000
Fixed Capital Investment	72600	71600	64500	61500	69600	79100	85700
Total Capital Investment	85400	84200	75900	72300	81800	93100	100800
Operating costs, k€/y							
Variable costs [a]	35016	34790	36535	36947	36365	35446	34406
Fixed costs [b]	10489	10367	9501	9135	10123	11282	12087
Capital charge, k€/y	8712	8592	7740	7380	8352	9492	10284
Total production costs, k€/y	54217	53749	53776	53462	54840	56220	56777
Total production costs, €/t $_{\text{biocrude}}$	659	564	529	465	538	450	1136
Total production costs, €/GJ $_{\text{biocrude}}$	20.5	17.0	16.5	14.1	16.8	13.6	35.1

[a] Variable costs include feedstocks, utilities, catalysts and wastewater treatment costs (See Table 7).

[b] Fixed costs include: labour, supervision, maintenance, local taxes, insurance and plant overhead costs (See Table 7).

use) was calculated as 13.1 $kgCO_2$-eq/$GJ_{\text{biojet-fuel}}$ and 13.2 $kgCO_2$-eq./$GJ_{\text{biojet-fuel}}$ for FE340 and W300 respectively as shown in Fig. 4A. For the former, biocrude upgrading has the highest contribution (34%) followed by raw material acquisition (25%) and their transport (20%), and then finally followed by biocrude oil production (14%) and product transportation (7%). For W300, biocrude oil production has the lowest contribution (2%), as a result of zero consumption of natural gas. However, in these two HTL cases, the biojet fuel produced may lead to a GHG emissions reduction of around 85% in comparison to the petroleum based jet fuel (see Fig. 4C). This value is significantly higher than the 60% potential GHG emissions reduction for an algae-based biojet fuel obtained via HTL at a wastewater treatment plant (*i.e.* 35.2 $kgCO_2$-eq/$GJ_{\text{biojet-fuel}}$) [44]. Other authors have also reported lower potential GHG emissions reduction for biojet fuel production via hydro-processing (40–60%) and pyrolysis (60–75%), and also higher potential GHG emissions reduction via Fischer-Tropsch (up to 89%) [45,46].

Furthermore, considering that the two HTL processes analysed produce significant amounts of steam, and assuming that excess steam could directly be used for heating in a nearby process, the GWP results might be reduced (by applying the system expansion approach) by 1.5 and 13.8 $kgCO_2$-eq/$GJ_{\text{biojet-fuel}}$ for FE340 and W300 respectively, as shown in Fig. 4B. A particular variable affecting significantly the GWP results is the electricity emissions factor. In the base case, the low-carbon intensive Swedish electricity mix was used. When the European electricity mix is used instead, the GWP results increase to 21.1 and 21.9 $kgCO_2$-eq/$GJ_{\text{biojet-fuel}}$ for FE340 and W300 respectively (see Fig. 4B).

Table 11
Technical performance indicators results for biojet fuel production from biomass.

Parameter, Units	FE340	W300
Overall yields, %		
Renewable jet fuel to biomass	10.4	8.1
Upgraded oil to biomass	26.6	20.3
Renewable jet fuel to biocrude	28.4	28.3
Upgraded oil to biocrude	70.9	70.9
Consumption		
Natural gas (for heating)[a], t/y	3727	1627
Natural gas (steam reforming), t/y	1933	1333
Electricity, MW	8.6	7.1
Cooling water, MW	16.2	14.4
Excess heat, MW	9.4	41.9
Energy efficiency, %	73	58
Upgraded oil "product mix" quality		
HHV, MJ/kg	49.3	49.3
LHV, MJ/kg	46.2	46.2
Oxygen content, wt%	0.1	0.1
Water content, wt%	0.2	0.2
Density at 15 °C, kg/L	0.77	0.77

[a] Aggregated natural gas consumption in furnace and reboiler of fractional distillation column.

Table 12
Composition of total production costs for biojet fuel production via HTL.

Element, Units	FE340	W300
Delivered equipment cost, k€		
Liquefaction plant	15600	14100
Upgrading facility	7700	6500
Hydrogen plant	16900	14400
Total equipment cost, k€	40200	35000
Fixed Capital Investment, k€	202600	176400
Total Capital Investment, k€	238400	207600
Production costs, k€/y		
Biomass feedstock	31667	31667
Natural gas	764	400
Electricity	4800	3969
Cooling water	130	115
Wastewater treatment	1862	2001
Liquefaction catalyst	660	0
Labour & supervision	1920	1920
Maintenance	12156	10584
Fixed charges	4052	3528
Capital charge	24312	21168
Plant overhead	9853	8753
Total production costs, k€/y	92175	84105
Total production costs, €/t $_{\text{product mix}}$	1040	1245
Total production costs, €/L $_{\text{product mix}}$	0.80	0.96

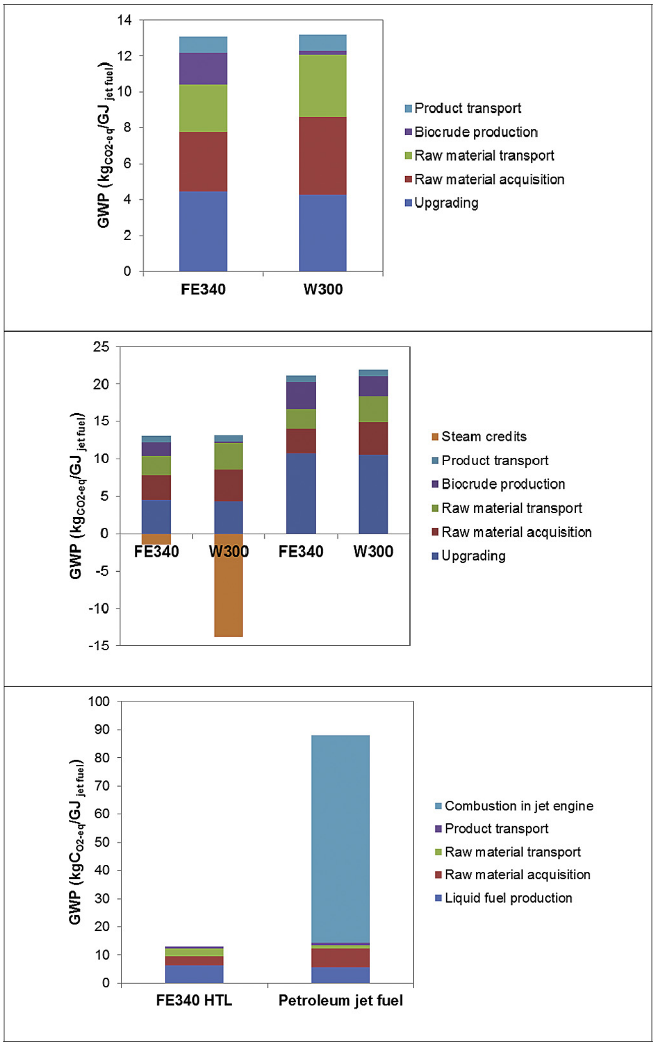

Fig. 4. Global warming potential results for: **A)** allocated biojet fuel GHG emissions via HTL; **B)** allocated biojet fuel GHG emissions via HTL incorporating: *i)* steam credits (columns on the left) and *ii)* the European electricity emission factor (columns on the right); **C)** Comparison of HTL FE340 jet fuel vs. petroleum jet fuel.

3.4. Sensitivity analysis

The biomass feedstock price and the liquefaction equipment costs have shown to have: *i*) strong effects on the process economics, and *ii*) large variability on data estimations. Thus, in order to analyse their influence on the overall economic performance of biojet fuel production, these two parameters are varied in the range ±50% as described in Section 2.8 to analyse their influence on the overall economic performance. As shown in Fig. 5, the total production costs are slightly more sensitive to changes on biomass price. Thus, a 50% decrease on the biomass price (from 95 to 47.5 €/dry tonne) will result on an 18% decrease on total production costs, while a similar reduction on the liquefaction costs (from 15.6 to 7.8 M€) results in a decrease of the total production costs of 10%. However, in both cases, the resulting production cost for the upgraded oil (862 and 932 €/$t_{\text{upgraded-oil}}$ respectively) is still significantly higher for fossil crude oil price 403 €/t [33].

4. Conclusions

The comparative analysis of techno-economic and GHG emissions performance for biojet fuel production via HTL, under different processing conditions (*i.e.* catalysts, temperature, and catalysts/biomass ratio) and based on detailed process simulation, showed that HTL may lead to higher yields, better energy efficiencies and lower processing costs than the more developed technology CP. However, the lowest production costs obtained for HTL biojet fuel (1086 €/$t_{\text{biojet-fuel}}$ or 25.1 €/$GJ_{\text{biojet-fuel}}$ via FE340) are double the commercial price of fossil jet fuel. This is still a significant economic gap that could partially be closed by further process optimization, or mass/heat integration, or by reducing operating costs related to raw materials and utilities. However, to achieve an economically competitive biojet fuel sector, additional (non-technological) measurements would be required, *e.g.* carbon emission taxes, or premium prices. This support could be justified due to the 85% GHG emissions reduction that HTL biojet fuel can offer with respect to those of fossil jet fuel. Furthermore, biomass HTL also co-produces gasoline, diesel and heavy oil, all of them with significantly lower GHG emissions than their fossil based counterparts. Future research should focus on further process and economic optimization of the full supply chain (including logistics) as well as on identifying non-technological measures and mechanisms that

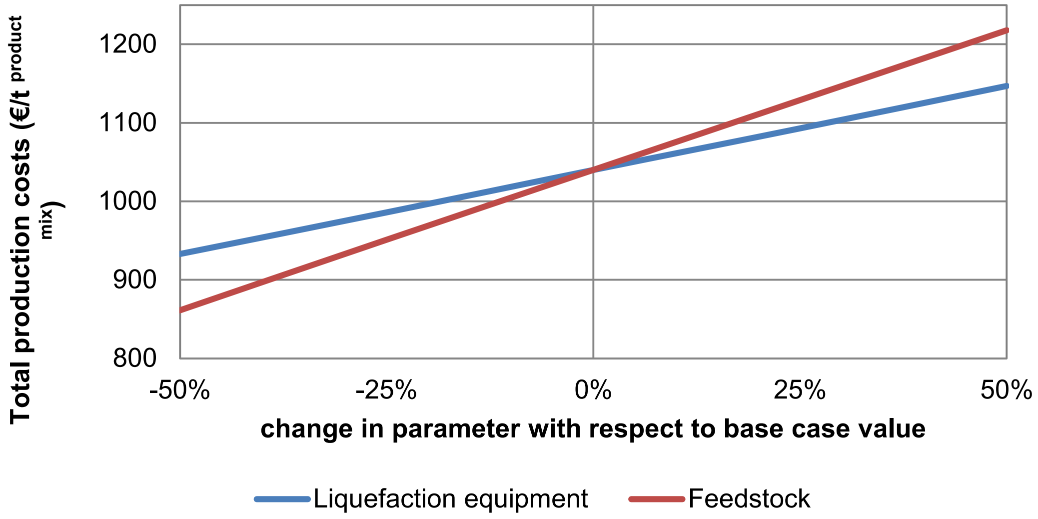

Fig. 5. Effect of liquefaction equipment and feedstock costs on total production costs per tonne of product mix. Base case values: biomass price 95 €/dry tonne; Liquefaction equipment costs 15.6 M€.

can further support the development of the biojet fuel sector.

Acknowledgements

This research was conducted as part of the Fuel Supply Chain Development and Flight Operations (RENJET) project, grant number APSP0002, which is funded by the EIT Climate-KIC. The core project partners (University of Utrecht, Imperial College London, SkyNRG, KLM, and Schiphol Airport) aimed to lay the basis for a self-sustaining network of regional renewable jet fuel supply chains based on sustainable (European) feedstock sources. The authors express their gratitude to dr. Ric Hoefnagels (UU) and Mr. Sierk de Jong (UU/SkyNRG) for their constructive feedback during the project.

References

[1] ICAO, ICAO: Annual Report of the Council 2012, International Civil Aviation Organisation (ICAO), 2013.

[2] EC. Aviation, European Commission Website, 2016. https://ec.europa.eu/clima/policies/transport/aviation/index_en.htm.

[3] M. Righi, J. Hendricks, R. Sausen, The global impact of the transport sectors on atmospheric aerosol in 2030 – Part 2: aviation, Atmos. Chem. Phys. 16 (2016) 4481–4495, http://dx.doi.org/10.5194/acp-16-4481-2016.

[4] S. de Jong, R. Hoefnagels, A. Faaij, R. Slade, R. Mawhood, M. Junginger, The feasibility of short-term production strategies for renewable jet fuels - a comprehensive techno-economic comparison, Biofuels, Bioprod. Bioref. 9 (6) (2015) 778–800.

[5] C.M. Alves, M. Valk, S. de Jong, A. Bonomi, L.A.M. van der Wielen, S.I. Mussatto, Techno-economic assessment of biorefinery technologies for aviation biofuels supply chains in Brazil, Biofuels, Bioprod. Bioref. (2016) 25, http://dx.doi.org/10.1002/bbb.1711.

[6] ATAG, Climate Change, 2015 [Online]. Available: http://www.atag.org/our-activities/climate-change.html (Accessed June 2015).

[7] U. Neuling, M. Kaltschmitt, Conversion routes for production of biokerosene - status and assessment, Biomass Convers. Bioref. 5 (4) (2014) 367–385.

[8] A. Demirbas, Competitive liquid biofuels from biomass, Appl. Energy (2011) 17–28,.

[9] T.R. Brown, A techno-economic review of thermochemical cellulosic biofuel pathways, Bioresour. Technol. 178 (2015) 166–176.

[10] F. Goudriaan, B. van de Beld, F.R. Boerefijn, G.M. Bos, J.E. Naber, S. van der Wal, J.A. Zeevalkink, Thermal efficiency of the HTU process for biomass liquefaction, in: Progress in Thermochemical Biomass Conversion, Tyrol, 2000.

[11] A. Veses, M. Aznar, I. Martínez, J.D. Martínez, J.M. López, M.V. Navarro, M.S. Callén, R. Murillo, T. García, Catalytic pyrolysis of wood biomass in an auger reactor using calcium-based catalysts, Bioresour. Technol. 162 (2014) 250–258.

[12] F. Behrendt, Y. Neubauer, M. Oevermann, B. Wilmes, N. Zobel, Direct liquefaction of biomass, Chem. Eng. Technol. 5 (2008) 667–677.

[13] J. Akhtar, N.A.S. Amin, A review on process conditions for optimum bio-oil yield in hydrothermal liquefaction of biomass, Renew. Sustain. Energy Rev. 15 (2011) 1615–1624.

[14] P. Sun, M. Heng, S. Sun, J. Chen, Direct liquefaction of paulownia in hot compressed water: influence of catalysts, Energy 35 (2010) 5421–5429.

[15] Y. Zhu, S.A. Tjokro Rahardjo, C. Valkenburg, L.J. Snowden-Swan, S.B. Jones, M.A. Machinal, Techno-economic Analysis for the Thermochemical Conversion of Biomass to Liquid Fuels, Pacific Northwest National Laboratory, Richland, 2011.

[16] P.M. Mortensen, J.-D. Grunwaldt, P.A. Jensen, K.G. Knudsen, J. A. D, A review of catalytic upgrading of bio-oil to engine fuels, Appl. Catal. A General 407 (2011) 1–19.

[17] K.F. Tzanetis, C.S. Martavaltzi, A.A. Lemonidou, Comparative exergy analysis of sorption enhanced and conventional methane steam reforming, Int. J. Hydrogen Energy 37 (2012) 16308–16320.

[18] P.J. Valdez, M.C. Nelson, H.Y. Wang, X.N. Lin, P.E. Savage, Hydrothermal liquefaction of Nannochloropsis sp.: systematic study of process variables and analysis of the product fractions, Biomass Bioenergy 46 (2012) 317–331.

[19] E. Panisko, E. Wietsma, T. Lemmon, K. Albrecht, D. Howe, Characterization of the aqueous fractions from hydrotreatment and hydrothermal liquefaction of lignocellulosic feedstocks, Biomass Bioenergy 74 (2015) 162–171.

[20] W.R. Niessen, Combustion and Incineration Processes Applications in Environmental Engineering, CRC Press, 2010.

[21] V. Ganapathy, Industrial Boilers and Heat Recovery Steam Generators, Marcel Dekker, Inc., 2003.

[22] S. Mani, S. Sokhansanj, X. Bi, A. Turhollow, Economics of producing fuel pellets from biomass, Appl. Eng. Agric. 22 (3) (2006) 421–426.

[23] M.M. Wright, D.E. Daugaard, J.A. Satrio, R.C. Brown, Techno-economic analysis of biomass fast pyrolysis to transportation fuels, Fuel 89 (2010) S2–S10.

[24] Y. Zhu, M.J. Biddy, S.B. Jones, D.C. Elliot, A.J. Schmidt, Techno-economic analysis of liquid fuel production from woody biomass via hydrothermal liquefaction (HTL) and upgrading, Appl. Energy 129 (2014) 384–394.

[25] E. Furimsky, Catalytic hydrodeoxygenation, Appl. Catal. A General 199 (2000) 147–190.

[26] S.K. Tanneru, P.H. Steele, Pretreating bio-oil to increase yield and reduce char during hydrodeoxygenation to produce hydrocarbons, Fuel 133 (2014) 326–331.

[27] P. Spath, A. Aden, T. Eggeman, R.M.B. Wallace, J. Jechura, Biomass to Hydrogen Production Detailed Design and Economics Utilizing the Battele Columbus Laboratory Indirectly- Heated Gasifier, NREL, 2005.

[28] T.P. Vispute, G.W. Huber, Production of hydrogen, alkanes and polyols by aqueous phase processing of wood-derived pyrolysis oils, Green Chem. 11 (2009) 1433–1445.

[29] W.D. Seider, J.D. Seader, D.R. Lewin, S. Widargo, Product and Process Design Principles, Synthesis, Analysis and Evaluation, John Wiley & Sons, Inc., 2010.

[30] M.S. Peters, K.D. Timmerhaus, R.E. West, Plant Design and Economics for Chemical Engineers, McGraw-Hill, 2004.

[31] R.K. Sinnot, Coulson & Richardson's Chemical Engineering, Butterworth-Heinemann, 1999.

[32] G. Towler, R. Sinnott, Chemical Engineering Design: Principles, Practice and Economics of Plant and Process Design, Butterworth-Heinemann, Oxford, 2012.

[33] Index Mundi, Commodity Prices, 2015 [Online]. Available: http://www.indexmundi.com/commodities/ (Accessed August 2015).

[34] P. Biller, Research on hydrothermal liquefaction for the production of aviation fuels, in: EUBCE, Vienna, 2015.

[35] I. Martínez, Basic and Applied Thermodynamics (Translated from Spanish), Dossat, 1992.

[36] DESTATIS, Press Releases - Labour Cost Comparison across EU Countries for 2014, 2015 [Online]. Available: https://www.destatis.de/EN/PressServices/Press/pr/2015/05/PE15_160_624.html (Accessed 2015).

[37] Bloomberg, Energy & Oil, 2015 [Online]. Available: http://www.bloomberg.com/energy (Accessed June 2015).

[38] Eurostat, Electricity Prices by Type of User, 2015 [Online]. Available: http://ec.europa.eu/eurostat/tgm/refreshTableAction.do;jsessionid=8eBEUL9Vf_pAGyT8f2JTnsjA9WYKoj7sfSTdNe4RTJjftBNde-_X!-1393835901?tab=table&plugin=1&pcode=ten00117&language=en (Accessed 2015).

[39] Alibaba, Alibaba.com, 2015 [Online]. Available: http://www.alibaba.com/ (Accessed June 2015).

[40] International Standards Organization (ISO), ISO 14040:2006, Environmental Management. Life Cycle Assessment. Principles and Framework, 2006.

[41] International Standards Organization (ISO), ISO 14044:2006, Environmental Management. Life Cycle Assessment. Requirements and Guidelines, 2006.

[42] P. Pawelzik, M. Carus, J. Hotchkiss, R. Narayan, S. Selke, M. Wellisch, M. Weiss, B. Wicke, M.K. Patel, Critical aspects in the life cycle assessment (LCA) of bio-based materials - reviewing methodologies and deriving recommendations, Resour. Conserv. Recycl. 73 (2013) 211–228.

[43] E. Searcy, P. Flynn, E. Ghafoori, A. Kumar, The relative cost of biomass energy transport, Appl. Biochem. Biotechnol. 137 (1–12) (2007) 639–652.

[44] M.-O.P. Fortier, G.W. Roberts, S.M. Stagg-Williams, B.S.M. Sturm, Life cycle assessment of bio-jet fuel from hydrothermal liquefaction of microalgae, Appl. Energy 122 (2014) 73–82.

[45] A. Elgowainy, J. Han, M. Wang, N. Carter, R. Stratton, J. Hileman, Life-cycle Analysis of Alternative Aviation Fuels in GREET, Argonne National Laboratory, 2012.

[46] J. Han, A. Elgowainy, H. Cai, M.Q. Wang, Life-cycle analysis of bio-based aviation fuels, Bioresour. Technol. 150 (2013) 447–456.